



ELSEVIER

Available online at [www.sciencedirect.com](http://www.sciencedirect.com)

SCIENCE @ DIRECT®

Optics Communications 251 (2005) 179–185

OPTICS  
COMMUNICATIONS

[www.elsevier.com/locate/optcom](http://www.elsevier.com/locate/optcom)

# All-optical variable-in variable-out wavelength converter based on cascaded nonlinearity in aperiodic optical superlattice

Wei Xie, Xianfeng Chen \*, Yuping Chen, Yuxing Xia

*Institute of Optics and Photonics, Department of Physics, The State Key Laboratory on Fiber Optic Local Area Communication Networks and Advanced Optical Communication Systems, Shanghai Jiao Tong University, 800 Dongchuan Rd. Shanghai 200240, China*

Received 30 September 2004; received in revised form 21 January 2005; accepted 21 February 2005

## Abstract

We theoretically report a new method to achieve variable-in, variable-out wavelength conversion in  $\text{LiNbO}_3$  with aperiodic optical superlattices (AOS) structure. The optimal structure of the  $\text{LiNbO}_3$  sample was obtained through simulated annealing method. About 3.4-nm prescribe pump bandwidth at 1559 nm is achieved to fulfill variable wavelength conversion among four selected ITU signal channels (C23–C20). As the result of large pump bandwidth, the reduced effective nonlinear coefficient of the AOS sample decreases to 0.21. Fluctuation of the operation temperature, variation of the incident angle and the errors in poling process show little influence on the performance of the device.

© 2005 Elsevier B.V. All rights reserved.

PACS: 42.65.J; 42.65.K

Keywords: Wavelength conversion; Quasi-phase-matching; Aperiodic optical superlattice

## 1. Introduction

Wavelength conversion, based on difference-frequency generation (DFG), is an attractive way

for realizing all-optical transparent network layer in the future wavelength division multiplexing (WDM) networks. It offers a series of novel features, such as ultra-high speed, large signal bandwidth, no excess noise and transparency to the bit-rate and data format [1]. However, the traditional birefringence-phase-matching (BPM) method suffers from low conversion efficiency and walk-off effect, which limits the further research of the DFG-based wavelength conversion.

\* Corresponding author. Tel.: +86 21 54743252; fax: +86 21 54743273.

E-mail addresses: [xieweixw@sjtu.edu.cn](mailto:xieweixw@sjtu.edu.cn) (W. Xie), [xfchen@sjtu.edu.cn](mailto:xfchen@sjtu.edu.cn) (X. Chen).

With the emergency of the quasi-phase-matching (QPM) technique, it is possible to fulfill expected wavelength conversion with relatively high efficiency and less restrictions. Effective QPM-based wavelength conversions have been demonstrated with periodically poled LiNbO<sub>3</sub> [2–4]. However, one distinct drawback of this kind of wavelength converters is that the QPM-bandwidth for the pump is very narrow. Thus, only a certain wavelength can be assigned to the pump, it follows that the converted wavelength is fixed if the signal wavelength is fixed. As a consequence, variable-in, variable-out wavelength conversions required in OXC networks cannot be achieved through the conventional QPM technique. Recently, some schemes for realizing variable-in, variable-out wavelength conversion are reported. One is MgO-doped LiNbO<sub>3</sub> QPM waveguide device [5], in which variable wavelength conversions in 1.5- $\mu\text{m}$  band were achieved by adjusting the operation temperature of the device to meet different QPM conditions. The other approaches are using phase-modulated structure [6,7] to realize multi-wavelength conversions. In the above approaches for wavelength conversion, fine adjustment of the operation temperature and wavelength accuracy are required owing to the narrow acceptance bandwidth for pump wavelength and operation temperature. Also, the recent development of broadband second harmonic generation (SHG) process [8,9] and cascaded nonlinearity [10–12] has been reported. The combination of cascaded nonlinear process and flattop SHG process can lead to the realization of all-optical variable-in variable-out wavelength conversion. Aperiodic domain-inverted structure can supply much more reciprocal vectors for multiple QPM than that of periodically poled crystals and has been employed to achieve multiple and broaden-band QPM process in the past years [13–15].

In this paper, we theoretically propose a new kind of wavelength converter based on cascaded second-order nonlinear process in LiNbO<sub>3</sub> with aperiodic optical superlattices (AOS) structure. It provides a broadened flattop bandwidth for the pump so that the wavelength converter can fulfill variable-in, variable-out wavelength conversion. Moreover, it offers relatively high efficiency and

large tolerance for the temperature, the incident angle and poling errors.

## 2. Theory of cascaded nonlinear process (SHG and DFG) in AOS

As shown in Fig. 1(a), the LiNbO<sub>3</sub> sample is divided into layers with the same thickness  $L_0$ , and the length of each layer  $L_0$  is less than the coherence length of the DFG process. The poling orientation of each layer, corresponding to the sign of nonlinear optical coefficient, can be determined through the simulated annealing (SA) method when we select an appropriate object function [15,16]. The arrangement of these layers is irregular so that the AOS structure can provide desirable reciprocal lattice vectors to meet the expected phase matching conditions, which is different from the situation of QPM periodic structure. After specified calculation, the optimal arrangement was chosen to achieve the prescribed broaden flattop bandwidth.

For simplicity, SHG process in bulk LiNbO<sub>3</sub> is used as an example to optimize the AOS structure in order to obtain the broad flattop bandwidth for fundamental wavelength. Since the tolerance of the signal wavelength is very large ( $\sim 60$  nm) [5], the optimal structure obtained based on SHG can be used to fulfill the variable wavelength conversion when adopting cascaded second-order nonlinear susceptibility  $\chi^{(2)}:\chi^{(2)}$  scheme. In this process, a pump beam in 1.5  $\mu\text{m}$  band is first converted into second harmonic (SH), and then the SH is used as the pump of the DFG process in order to obtain the converted wave. In terms of mathematic, it can be expressed as:  $\omega_c = 2\omega_p - \omega_s$ , where  $\omega_c$  is the frequency of the converted wave,  $\omega_p$  is the pump and  $\omega_s$  is the signal, respectively.

We assume that a laser beam with the wavelength of  $\lambda_p$  is perpendicularly incident from the left side of the sample and thereafter the second harmonic field is generated. Under the slowly varying amplitude and the small-signal approximation, the amplitude of the fundamental wave can be treated as constant along the interaction length. As a result, the amplitude of the second

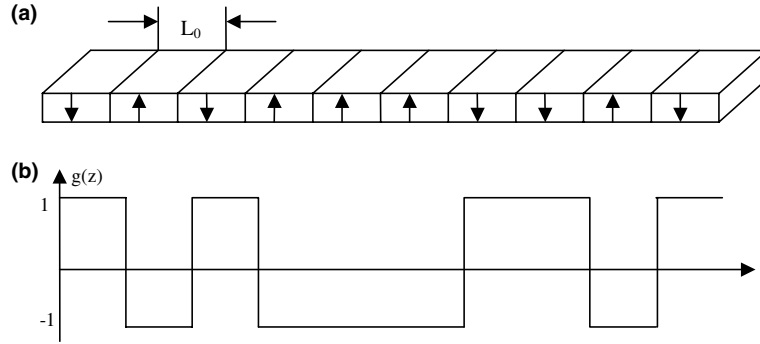


Fig. 1. (a) Schematic diagram of an aperiodic-optical-superlattice grating in part. (b) Normalized structure function  $g(z)$ .

harmonic field at the end of the AOS grating can be expressed as [17]:

$$E_{\text{SHG}}(\lambda_p) = i \frac{\omega_p}{n_{\text{SHGC}}} E_p^2 \int_0^L d(z) \exp[-i\Delta k(\lambda_p)z] dz, \quad (1)$$

where  $E_p$  and  $E_{\text{SHG}}$  are the field amplitudes of the fundamental and harmonic waves, respectively;  $n_{\text{SHGC}}$  is the refractive index at harmonic wavelength  $\lambda_{\text{SHG}}$ ;  $\omega_p$  is the frequency of the fundamental wave.  $\Delta k(\lambda_p) = k_{\text{SHG}} - 2k_p = \pi/l_c(\lambda_p)$ , where  $l_c(\lambda_p)$  is the coherence length.  $d(z)$  is the nonlinear coefficient of the lithium niobate with AOS structure.  $L = NL_0$  is the total length of the AOS grating,  $N$  is the number of the layers and  $L_0$  is the length of the individual layer.

When the polarizations of the fundamental and second harmonic wave are all along  $C$ -axis (i.e., extraordinary wave), the SHG process utilizes the largest component of the nonlinear coefficient tensor  $d_{33}$ . A new normalized function  $g(z) = d(z)/d_{33}$  is introduced as the structural function of the aperiodic domain-inverted  $\text{LiNbO}_3$  [18]. Obviously,  $g(z)$  only takes the binary values of  $\pm 1$  in AOS grating (Fig. 1(b)). Thus, (1) can be rewritten as:

$$E_{\text{SHG}}(\lambda) = iL \frac{\omega_p}{n_{\text{SHGC}}} E_p^2 d_{33} G(\lambda), \quad (2)$$

$$G(\lambda) = \frac{1}{L} \int_0^L g(z) \exp[-i\Delta k(\lambda)z] dz. \quad (3)$$

As shown in (2), the conversion efficiency of the SHG process depends on the normalized structure function  $g(z)$  and is proportional to  $|G(\lambda)|^2$ . In

terms of Fourier transform,  $G(\lambda)$  is the spectrum function in the wave-vector mismatch  $\Delta k$  domain of the space-dependent nonlinear coefficient function  $g(z)$  in the space domain. Compared with  $d_{33}$  for the perfect phase-match process, the effective nonlinear coefficient in AOS is  $d_{\text{eff}} = G(\lambda)d_{33}$ .

Once the SH is generated, the other nonlinear process DFG is started, where the SH wave and the signal interact to produce an output wave at the difference-frequency  $\omega_c = 2\omega_p - \omega_s$ . If the wavelength of signal  $\lambda_s$  is close to the pump wavelength  $\lambda_p$ ,  $k_s + k_c$  is approximately equal to  $2k_p$ , where  $k_s$ ,  $k_p$ ,  $k_c$  are the wave-vector of the signal, pump and converted wave in  $\text{LiNbO}_3$ , respectively. Therefore, the DFG phase-match condition will be satisfied if we realize the SHG phase-match condition in AOS sample. Obviously, the signal, pump, SH and converted wave interact in the  $\text{LiNbO}_3$  crystal, which is known as wave mixing process. Based on the couple-wave equation, assumption that the fundamental wave in SHG process is a constant in the interaction and the small-signal approximation, we obtain the equations as follows:

$$\begin{cases} \frac{dE_s}{dz} = \frac{8\pi\omega_s^2 d}{k_s c^2} E_p E_c^* e^{i\Delta k z}, \\ \frac{dE_c}{dz} = \frac{8\pi\omega_c^2 d}{k_c c^2} E_p E_s^* e^{i\Delta k z}, \\ \frac{dE_p}{dz} = \frac{8\pi\omega_p^2 d}{k_p c^2} E_c E_s e^{-i\Delta k z}. \end{cases} \quad (4)$$

Generally, we can only obtain the numerical solutions of the equations. When the phase-match conditions of the SHG and DFG processes are satisfied, the mismatch of wave-vector  $\Delta k \approx$

$\Delta k_{\text{SHG}} \approx \Delta k_{\text{DFG}} = 0$ . With the assumption of low efficiency condition, we obtain the conversion efficiency of the cascaded process:

$$\eta = \frac{P_c}{P_s} = \frac{1}{4} j_{\text{norm}} d_{\text{eff}}^4 L^4 P_p^2, \quad (5)$$

where  $j_{\text{norm}}$  is a coefficient determined by the wavelength of the signal, pump and converted wave. Here, the effective nonlinear coefficient  $d_{\text{eff}} = G(\lambda) d_{33}$ .

Consequently, we introduce a new function  $d_{\text{reff}} = |G(\lambda)|$  to study the conversion efficiency, where  $d_{\text{reff}}$  refers to the reduction in effective nonlinearity comparing with that for the perfect phase-match process [19]. In the case of periodic structure of conventional QPM,  $d_{\text{reff}}$  is calculated to be  $2/\pi$  (0.6366).

### 3. Simulation results and discussions

In our simulations, we adopt the length of each layer  $L_0 = 3 \mu\text{m}$ , and  $N = 3300$ . Thus, the total length of the grating  $L$  is 9.9 mm. Moreover, the refractive indices of the fundamental and second harmonic depend on the Sellmerier equation and the operation temperature of the sample is assigned to be 23 °C [20]. We take International Telecommunication Union (ITU) grid channels C20–C23 (C20:1561.42 nm; C21:1560.61 nm; C22:1559.79 nm; C23:1558.98 nm) as the signal wavelengths. In order to achieve variable wavelength conversions among the four channels, we pre-design the broadened flattop bandwidth for 3.4 nm around 1559 nm in our simulation.

Choosing a proper object function in the SA method, we obtain the optimal structure of the AOS sample. Then, we scan the sample with signal wavelength from 1550 to 1570 nm with the step of 0.1 nm. The calculation result is shown in Fig. 2, the pre-designed large bandwidth desired in DFG-based wavelength conversion is achieved in LiNbO<sub>3</sub> with AOS structure.

As shown in Fig. 2, the desired broadened flat-top is achieved through SA method. Six pump wavelengths ( $\lambda_{12}$  (1559.4 nm),  $\lambda_{13}$  (1559.8 nm),  $\lambda_{14} = \lambda_{23}$  (1560.2 nm),  $\lambda_{24}$  (1560.6 nm) and  $\lambda_{34}$  (1561 nm)) needed in wavelength conversions

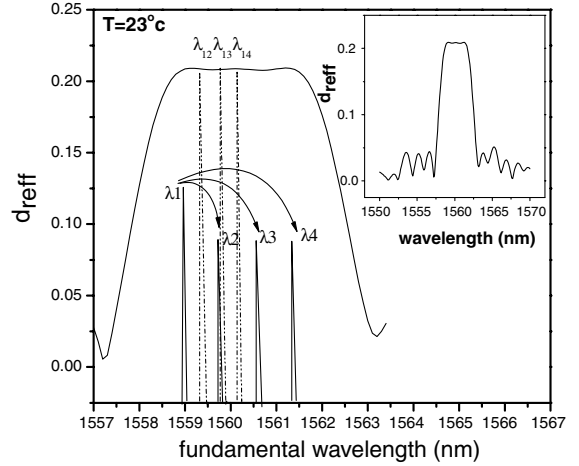


Fig. 2. The calculated conversion spectra based on the AOS gratings and the wavelength conversions based on DFG from C23 to the other three channels with different pump wavelengths. (where the  $\lambda_1$ ,  $\lambda_2$ ,  $\lambda_3$ ,  $\lambda_4$  represent the wavelength of four signal channels: C23, C22, C21, C20 and  $\lambda_{12}$ ,  $\lambda_{13}$ ,  $\lambda_{14}$  are the pump wavelength.). The insert is the whole calculated broadened flattop bandwidth for fundamental wavelength.

among the four signal channels are covered by the flattop bandwidth. It follows that the variable wavelength conversion among the four channels can be fulfilled with relatively high effective nonlinear coefficient ( $d_{\text{reff}}$ ). The wavelength conversions from  $\lambda_1$  (C23: 1558.98 nm) to the other three channels (C22–20) with different pump wavelength:  $\lambda_{12}$ ,  $\lambda_{13}$  and  $\lambda_{14}$  are demonstrated in Fig. 2. In the same way, we can also realize this kind of variable wavelength conversion with the other three channels (C22–20). The reduced effective nonlinear coefficient ( $d_{\text{reff}}$ ) in the interaction process is about 0.21 and the flattop width is about 3.4 nm. In the case of the perfect QPM periodic structure with the same length of 9.9 mm, the reduced effective nonlinear coefficient and the bandwidth are  $2/\pi$  (0.6366) and 0.95 nm. We find that an over decuple pump bandwidth is achieved only at the expense of 66% reduction of the effective nonlinear coefficient. As demonstrated above, the large pump bandwidth can be engineered in LiNbO<sub>3</sub> when adopting AOS structure. As we know, optical superlattice with shorter length will result in lower conversion efficiency but larger bandwidth. For example, 3.3-mm length device provides about 3 nm bandwidth

and effective nonlinear coefficient is about  $(2/3\pi)d_{33}$ . Comparing it with the AOS structure, we can find AOS structure provides about 4.8-nm half-width (flattop width 3.4 nm) at almost the same efficiency. In addition, same conversion efficiency within the flattop can be achieved.

In our calculations, the relation between the central wavelength of the broadened flattop bandwidth and temperature attracts our attention. With the variation of the temperature, the central wavelength of the flattop shifted while the shape of the broadened flattop doesnot change. As a consequence, this variation of the central wavelength can be used to change the operation wave band of the wavelength converter. The temperature dependency of the central wavelength is shown in Fig. 3, where we scan the AOS grating from 10 to 200 °C with a step of 10 °C. As shown in Fig. 3, the central wavelength of the broad flattop depends linearly on the temperature and the tuning rate of temperature for fundamental wavelength is approximately 0.14 nm/°C. It follows that this kind of wavelength converter can also be used to fulfill the variable wavelength conversion in different wave band by changing the operation temperature of the device.

As illustrated above, the fluctuation of the operation temperature causes the fluctuation of the central wavelength but doesnot change the shape

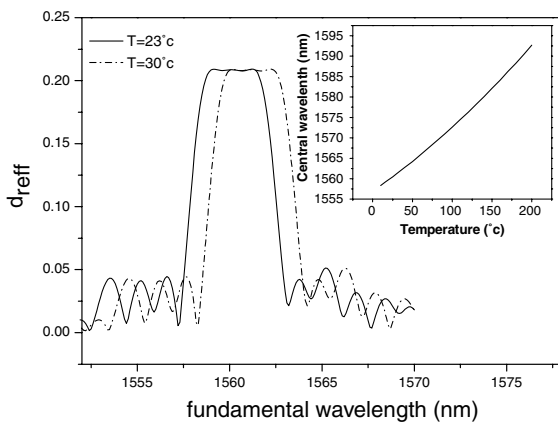


Fig. 3. The broadened flattop pump bandwidth shifts as the temperature changes while the whole profile doesnot change. The insert is the temperature dependency of the central wavelength of the broad bandwidth.

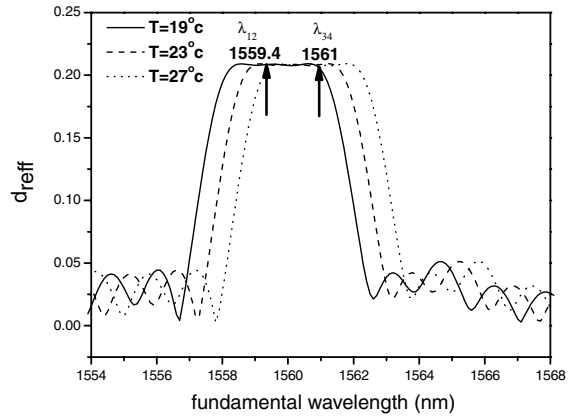


Fig. 4. The tolerance of the operation temperature. The six desired pump wavelengths stay in the flattop in spite of the variation of the operation temperature. The tolerance bandwidth for the operation temperature is about 8 °C.

of the broadened flattop. As long as the six pump wavelength still stay in the broadened flattop, the wavelength conversion can be fulfilled with the same effective nonlinear coefficient: 0.21. In Fig. 4, although the operation temperature varies from 19 to 27 °C, the desired pump wavelengths  $\lambda_{12}$  (1559.4 nm),  $\lambda_{13}$  (1559.8 nm),  $\lambda_{14} = \lambda_{23}$  (1560.2 nm),  $\lambda_{24}$  (1560.6 nm) and  $\lambda_{34}$  (1561 nm) for mutual wavelength conversions still stay in the broaden flattop due to the pre-designed larger pump bandwidth of 3.4 nm. Therefore, the variable wavelength conversions can still be achieved with expected efficiency. When the temperature is beyond the range of 19–27 °C, the conversion efficiency will decrease. The tolerance bandwidth for the temperature is about 8 at 23 °C. It can be concluded that the device can work properly in spite of the slight fluctuation of the temperature.

Similar to the influence of temperature fluctuation, the variation of incident angle also caused the change of the central wavelength but doesnot alter the profile of the broadened flattop. The calculation result is shown in Fig. 5 at the temperature of 23 °C. As the incident angle changes from 0° to 7°, the central wavelength changes consistently but the six desired pump wavelength still stay in the broaden flattop. Therefore, the tolerance bandwidth for the incident angle is about 7° at the temperature of 23 °C.

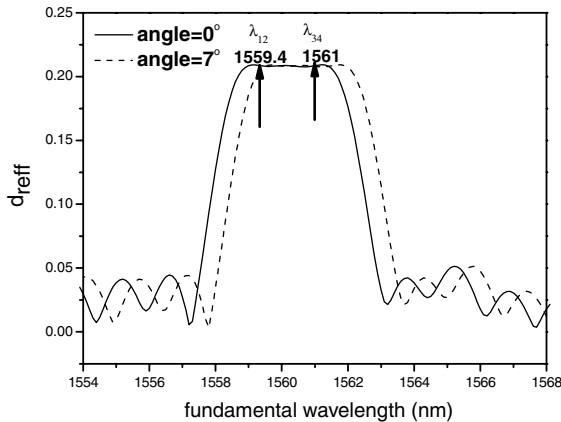


Fig. 5. The tolerance of the incident angle. The six desired pump wavelength stay in the flattop in spite of the variation of the incident angle. The tolerance bandwidth for the incident angle is about  $7^\circ$ .

As it is well known, under current room-temperature poling technique, the inverted domains possibly grow beyond the width of the metal electrode. The error of domain length is unavoidable. We consider the resultant domain size after the poling process as follows: (1) the inverted domains may extend its edge into adjacent layers and the un-inverted domains are shortened; (2) the

inverted domains do not reach their pre-designed edges so that the un-inverted domains are consequently lengthened. We define  $u$  as the length of the errors and the sign of  $u$  as the direction of the extension, where  $+$  represents that the inverted domains extend to the un-inverted domains and vice versa. The calculation results are shown in Fig. 6. The length of each layer in our calculations is  $3 \mu\text{m}$ , we take the poling error  $u = 0, +1, +2 \mu\text{m}$  (left in Fig. 6) and  $u = 0, -1, -2 \mu\text{m}$  (right in Fig. 6) for comparison. Obviously, the effective nonlinear coefficient and the quality of the broadened flattop decrease as the absolute value of  $u$  increases. When the error of the domain is not large enough, it shows a little influence on the performance of the device, which is practically favorable for practical application.

#### 4. Conclusions

In summary, we have theoretically proposed a kind of wavelength converter in lithium niobate crystal with AOS structure. Broadened flattop bandwidth for wavelength conversion is achieved in AOS so that the variable-in, variable-out wavelength conversions can be realized. The device

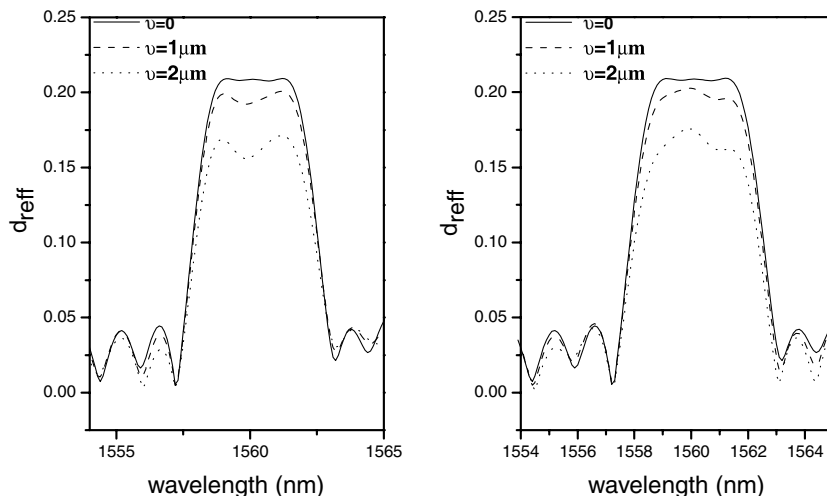


Fig. 6. The influence of domain errors on the performance of the wavelength conversions. The left (right) shows the calculation results while the inverted domains extend to adjacent domains (the inverted domains do not reach its pre-designed edge). The effective nonlinear coefficient decrease with the poling error increase.

can provide relatively large tolerance for the operation temperature and incident angle. The calculations also show that the errors of domain length in poling process have little influence on the performance of the device. Therefore, the variable wavelength conversion based on AOS structure may be a new promising approach for variable wavelength conversion desired in future OXC networks.

### Acknowledgments

This research was supported by the National Science Foundation of China (No. 60477016), the Foundation for Development of Science and Technology of Shanghai (Nos. 02DJ14001 and 04DZ14001), and the “Shu-Guang” Scholar Plan of Shanghai Education Committee.

### References

- [1] S.J.B. Yoo, *J. Lightwave Technol.* 14 (1996) 955.
- [2] Xianglong Zeng, Xianfeng Chen, *Opt. Laser Technol.* 35 (2003) 187.
- [3] M.H. Chou, I. Brener, M.M. Fejer, E.E. Chaban, S.B. Christman, *IEEE Photonic. Tech. Lett.* 11 (1999) 653.
- [4] M.H. Chou, J. Hauden, M.A. Arbore, M.M. Fejer, *Opt. Lett.* 23 (1998) 104.
- [5] Bo Chen, Chang-Qing Xu, Bing Zhou, *OFC THDD2* (2002) 593.
- [6] Masaki Asobe, Osamu Tadanaga, Hiroshi Miyazawa, Yoshiki Nishida, Hiroyuki Suzuki, *Opt. Lett.* 28 (2003) 558.
- [7] M.H. Chou, K.R. Parameswaran, M.M. Fejer, *Opt. Lett.* 24 (1999) 1157.
- [8] M.L. Bortz, M. Fujimura, M.M. Fejer, *Electron. Lett.* 30 (1994) 34.
- [9] K. Mizuuchi, K. Yamamoto, M. Kato, H. Sato, *IEEE J. Quantum Elect.* 30 (1994) 1596.
- [10] G.I. Stegeman, D.J. Hagan, L. Torner, *Opt. Quant. Electron.* 28 (1996) 1691.
- [11] H. Kanbara, H. Itoh, M. Asobe, K. Noguchi, H. Miyazawa, T. Yanagawa, I. Yokohama, *IEEE Photonic. Tech. Lett.* 11 (1999) 328.
- [12] H. Ishizuki, T. Suhara, M. Fujimura, H. Nishihara, *Opt. Quant. Electron.* 33 (2001) 953.
- [13] Y.W. Lee, F.C. Fan, Y.C. Huang, B.Y. Gu, B.Z. Dong, M.H. Chou, *Opt. Lett.* 27 (2002) 2191.
- [14] Katia Gallo, Gaetano Assanto, George I. Stegeman, *Appl. Phys. Lett.* 71 (1997) 1020.
- [15] Ben-Yuan Gu, Bi-Zhen Dong, Yan Zhang, Guo-Zhen Yang, *Appl. Phys. Lett.* 75 (1999) 2175.
- [16] S. Kirkpatrick, C.D. Gelatt, M.P. Vecchi, *Science* 220 (1983) 671.
- [17] Martin M. Fejer, G.A. Magel, Dieter H. Jundt, Robert L. Byer, *IEEE J. Quantum Elect.* 28 (1992) 2631.
- [18] Xianglong Zeng, Xianfeng Chen, *Opt. Commun.* 204 (2002) 407.
- [19] Ben-Yuan Gu, Yan Zhang, Bi-Zhen Dong, *J. Appl. Phys.* 87 (2000) 7629.
- [20] D.H. Jundt, *Opt. Lett.* 22 (1997) 1553.